# PARTICLE IMAGE VELOCIMETRY AND THERMOMETRY USING THERMOCHROMIC LIQUID CRYSTALS

**Tomasz A. KOWALEWSKI**

*IPPT PAN, Polish Academy of Sciences*
*Center of Mechanics and Information Technology*
*Swietokrzyska 21, PL - 00049 Warszawa*

## Summary

*In recent years Thermochromic Liquid Crystals (TLCs) have been successfully used in non-intrusive heat transfer and fluid mechanics studies. Application of TLC tracers allows instantaneous measurement of the temperature and velocity fields for two-dimensional cross-section of flow. Here we present the review of the development of techniques for visualising and analysing flow images with TLC tracers we used over past 15 years for studying natural convection in small enclosures. Using digital acquisition technique and image analysis methods, fully automatic quantification of temperature and velocity can be performed. The method combines computerised true-colour analysis of digital images for temperature measurements and modified Particle Image Velocimetry used to obtain the flow field velocity. Examples given for flow field measurements demonstrate advantages of the method and the importance of this full field experimental technique for the validation of numerical codes.*

## 1. Introduction

Liquid crystals are highly anisotropic fluids that exist between the boundaries of the solid phase and the conventional, isotropic liquid phase [20]. The TLCs based temperature visualisation is based on the property of some cholesteric and chiral-nematic liquid crystal materials to reflect definite colours at specific temperatures and viewing angle. The colour change for the TLCs ranges from clear at ambient temperature, through red as temperature increases and then to yellow, green, blue and violet, turning to colourless (isotropic) again at a higher temperature. Hence, liquid crystals used as temperature indicators modify incident white light and display colour whose wavelength is proportional to temperature. They can be painted on a surface or suspended in the fluid and used to make visible the distribution of temperature.

Normally clear, or slightly milky in appearance, liquid crystals change their colour over a narrow range of temperature. The displayed colour is red at the low temperature margin of the colour-play interval and blue at the high end. The colour-temperature play interval depends on the TLC composition. It can be selected for bands of about 0.5$^{o}$C to 20$^{o}$C and working temperature of -30$^{o}$C to above 100$^{o}$C. These colour changes are repeatable and reversible as long as the TLCs are not physically or chemically damaged. This being the case, they can be calibrated accurately with proper care and used in this way as temperature indicators.

Pure liquid crystal materials are thick, viscous liquids, greasy and difficult to deal with under most heat transfer laboratory conditions. The TLCs material is also sensitive to mechanical stress [2]. A micro-encapsulation process which encloses small portions of liquid crystal material in polymeric material was introduced to solve problems with the stress sensitivity as well as with the chemical deterioration.

During the past, liquid crystals have been extensively applied to the qualitative visualisation of entire steady state or transient temperature fields on solid surfaces [5,12,19,23]. Since quantifying colour is a difficult and somewhat ambiguous task, application of thermochromic liquid crystals initially was largely qualitative. Application of the colour films or interference filters was tedious and inaccurate. Only after employment of CCD colour camera and digital

image processing qualitative and fast temperature measurements became possible. The rapid development of the hardware and software image processing techniques make now possible to setup inexpensive systems capable of real-time transient full field temperature measurements using TLCs.

For flow analysis the suspension of thermochromic liquid crystals can be used to make visible the temperature and velocity fields in liquids [7]. By dispersing the liquid crystal material into the liquid they become not only classical tracers for flow visualisation but simultaneously small thermometers monitoring local fluid temperature. The typical diameter of the TLC tracers used is 50μm. With the density closed to that of water, TLC tracers are well conveyed by the flow of liquids. Their response time is about 10ms, which is short enough for typical thermal problems in fluids.

A collimated source of white light must be used to illuminate selected cross-sections of the flow (light sheet technique) and colour images are acquired at the perpendicular direction. Figure 1 illustrates properties of the TLCs used as tracers to visualize flow structure. The characteristic spiralling motion in a differentially heated cube shaped cavity [9,10] can be easily identified. The colour of tracers apparently indicates distribution of the liquid temperature.

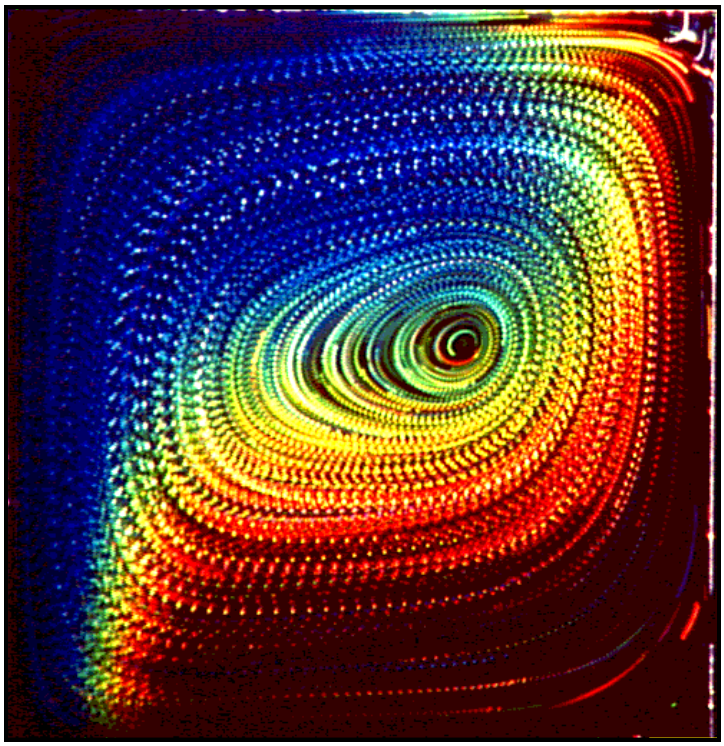

***Figure 1***. *Multiexposed colour photograph of the convective flow in glycerol seeded with liquid crystal tracers in a differentially heated cavity. Tracers change colour from blue to red following the clock-wise flow circulation from the hot wall (left) to the cold wall (right); temperature difference* $DT=4^{o}C$, $Ra=1.1\cdot10^{4}$, $Pr=6900$

In the above and following examples the unencapsulated TLCs tracers have been applied to measure both temperature and velocity flow fields. We found that light scattered by the capsule shell inevitable diminishes saturation of the observed colours. Because of the slow motion studied, the stress effects are negligible and fine dispersed raw material could be applied directly in our flow measurements.

In the following we illustrate several applications of TLC tracers to study natural convection of liquids in closed cavities also with phase change (freezing of water). In conjunction with the

experimental program, numerical simulations of the problem have been performed using finite difference models of the Navier-Stokes and energy equations [4,22]. The significance of the full field temperature and flow measurements for verification of the numerical results becomes evident by a direct comparison of the evaluated and predicted fields.

## 2. Flow field measurements

### 2.1. Particle Image Thermometry

TLCs are widely used to map temperature distributions on surfaces [5]. Application of TLC tracers to flow problems [6], combined with digital image analysis, gave impulse to quantitative and fully automatic temperature and velocity evaluation, based on Digital Particle Image Velocimetry (DPIV) [21] and Digital Particle Image Thermometry (DPIT) [3]. In the present study, use of both digital evaluation techniques, as initiated by Hiller et al. [11], allows us simultaneous and fully automatic measurements of temperature and velocity fields for selected 2-D flow cross-sections.
The temperature measurements are based on digital colour analysis of *RGB*[1] images. The *RGB* representation of the colour can be transformed to other *trichromic decomposition*. The choice of the colour space is not unique; several standards have been developed, especially for the colour television or printing applications. For evaluating the temperature so called *HSI*[2] representation of the *RGB* colour space is the most favourable. The hue (*chromaticity*) represents the dominant wavelength of the colour, i.e. the value which depends directly on the TLCs temperature. The light intensity (or brightness) is defined simply as a sum of its three primary components:

$$I = \sqrt{(R^2 + G^2 + B^2)} \,/\sqrt{3}$$

In our 8-bit representation the maximum intensity is equal to 255. Saturation represents colour purity. It can be easily found as a remainder after subtraction of the white background from the light intensity:

$$S = 255 \cdot (1 - \min(R,G,B) \,/\, I)$$

Pure colours have saturation equal to 255. The hue value is calculated as a normalized value of the dominating colour. To make use of the 8-bit signal dynamics and limiting ourselves to the spectral colours [6,13], the following formula is used to calculate the hue value:

$$H = \begin{cases} 63 + ((G'-R') \cdot 63) \,/\, (G'+R') & for \quad B' = 0 \\ 189 + ((B'-G') \cdot 63) \,/\, (G'+B') & for \quad R' = 0 \end{cases}$$

where: $R' = R - \min(R,G,B)$, $G' = G - \min(R,G,B)$ and $B' = B - \min(R,G,B)$.

The incoming *RGB* signals from the video camera are transformed pixel by pixel into hue, saturation and intensity. The red, green and blue colours correspond to the hue values of 0, 126 and 252, respectively. The temperature is determined by relating the hue to a temperature calibration function. Our 8-bit representation of the hue value ensures resolution better than

[1] Red, Green and Blue intensities produces by a video camera
[2] Hue, Saturation and Intensity

1%. However, the colour-temperature relationship is strongly non-linear. Figure 2 illustrates an example of the calibration curve obtained for the TLC tracers used in studying natural convection in freezing water. The selected colour play range covers temperatures from about $2^oC$ to $6^oC$. Due to non-linearity of the curve, the accuracy of the measured temperature depends on the colour (hue) value. The relative error, based on the temperature range defined by the TLCs colour-play limits, varies from 3% to 10%. For the TLCs used (TM from Merck) there results an absolute accuracy of $0.15^oC$ for lower temperatures (red-green colour range) and $0.5^oC$ for higher temperatures (blue colour range). The most sensitive region is the colour transition from red to green; it takes place for a temperature variation of less than one degree Celsius. To improve the accuracy of temperature measurements, some experiments were repeated using up to four different types of TLCs, so that their combined colour-play range could cover an extended temperature range.

Application of the TLCs for the phase change problems [14-16] yields several additional experimental constrains. The investigated temperature range is well defined by the phase change temperature. Hence the colour-play properties of the TLC material have to be correctly matched. In addition, the solidus surface generates additional light scattering and reflections. These may generate unexpected colour shifts or/and image distortions in regions next to the phase front and have to be accounted for throughout the calibration procedure.

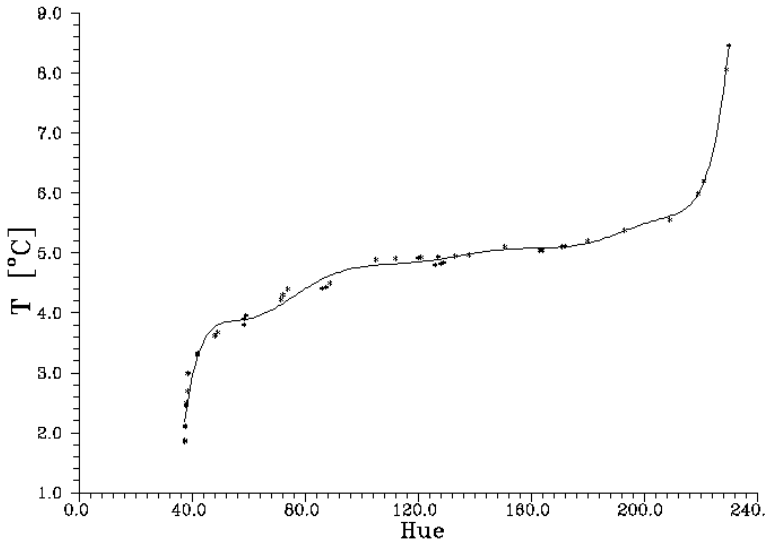


***Figure 2.*** *Temperature vs. Hue for TLCs sample used to study natural convection of water with freezing. Calibration curve obtained by $8^{th}$ order polynomial fitted to the experimental points*

Comparing to surface thermography, the use of TLC as dilute suspension in a fluid bears additional problems. First of all, the colour images of the flow are discrete, i.e. they represent a non-continuous cloud of points. Secondly, due to the secondary light scattering, its reflections from the side walls and internal cavity elements, the overall colour response may be distorted. Hence, the use of specifically developed averaging, smoothing and interpolating techniques are indispensable to remove ambiguity in the resulting isotherms. Further, every experimental set-up needs its own calibration curve obtained from the images using the same fluid, at the same illumination, acquisition and evaluation conditions.

The colour of light refracted by TLCs also depends on the observation angle. Our investigations [8] have shown that this relation is linear with slope equal to $0.07^oC$ per $10^o$ change of the angle. Therefore, it is important that the angle between the illuminated plane (light sheet plane) and the camera is fixed and that the viewing angle of the lens is small. In the

typical experiment, the flow was observed at $90^o$ with a 50mm lens and a 1/3' sensor, i.e. the camera viewing angle was smaller than $4^o$.

### 2.2. Particle Image Velocimetry

The 2-D velocity vector distribution has been measured by digital particle image velocimetry. By this method, the motion of the scattering particles, observed in the plane of the illuminating light sheet, is analysed. For this purpose, the colour images of the TLC tracers are transformed to black & white intensity images. To improve contrast and particles visibility a special filtering technique is applied. It allows to obtain bright images of the tracers, well suited for DPIV. The method is based on local analysis of the average intensity within small (3x3 pixel) windows. Pixels with intensity well above the average are treated as particles and their intensity is amplified. In such a way, bright images of the tracers with preserved intensity variation, well suited for DPIV, are obtained.

In the classical DPIV analysis, the magnitude and direction of the velocity vectors are determined using a FFT-based cross-correlation analysis between small sections (interrogation windows) of one pair of images taken at the given time interval. The average particle displacement during a given time interval determines the velocity vector representing the section investigated. Through a moving (step by step) interrogation window across the image, about 1000 vectors per one pair of images are obtained. The spatial resolution of the method is limited by the minimum number of tracers present in the interrogation window. In practice, only windows larger than 32x32 pixels are applicable. On the other hand, the dimension of the interrogation window limits the maximum detectable displacement. Hence, to improve the accuracy and dynamics of the velocity measurements, short sequences of images have been taken at every time step. The cross-correlation analysis performed between different images of the sequence (time interval between pairs changes) allows us to preserve similar accuracy for both the low and high velocity flow regions.

For some experimental data, the newly developed ODP-PIV[3] method [17] of image analysis has been also used to obtain dense velocity fields of improved accuracy. In the cited paper results of several accuracy tests performed for artificial images are given. It came out that for typical experimental conditions, i.e. images with 5% noise added and 5% particle disappearance, the accuracy of the „classical" FFT-based DPIV and that of the ODP-PIV method is 0.6 pixels and 0.15 pixels, respectively. It means that for typical displacement vector of 10 pixels the relative accuracy of the velocity measurement (for single point) is better than 6%.

To get a general view of the flow pattern, several images recorded periodically within a given time interval have been added in the computer memory. Displayed images are similar to the multiexposed photographs, showing the flow direction and its structure. This type of visualisation is very effective in detecting small re-circulation regions, usually difficult to identify in the velocity field. In all cases studied the volume concentration of tracers was very low (below 0.1%), so their effect on the flow and the physical properties of fluid was negligibly small.

[3] Orthogonal Dynamic Programming - Particle Image Velocimetry

## 3. Experimental details

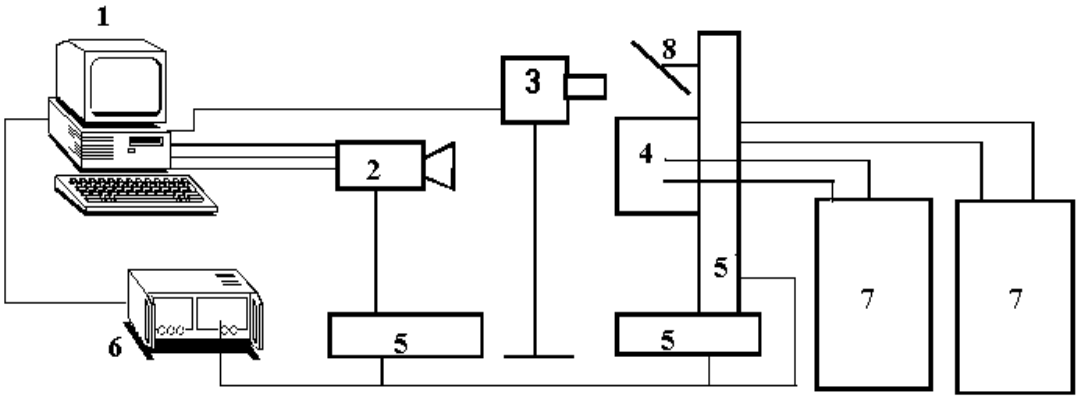


***Figure 3.*** *Schematic of the experimental system. PC (1) with the acquisition card controlling RGB camera (2), halogen lamp (3) and three stepping motors (5) using driver (6). Temperature in the cavity (4) controlled by two thermostates (7); mirror (8) used to direct light sheet*

The typical experimental setup used for the flow measurements consists of a convection box, a halogen tube lamp, the 3-chip CCD colour camera and the 32-bit frame grabber (Fig. 3). The flow field is illuminated with a 2mm thin sheet of white light from a specially constructed halogen lamp or xenon-flash tube and observed in the perpendicular direction. The 24-bit colour images, typically of 768x564 pixels, have been acquired with a personal computer. Using PCI based colour frame grabber (AM-STD ITI) and a 64MB Pentium computer, our setup permits us to gain in real time over 50 RGB images, before they have to be saved on the computer magnetic disk. The computer controls the system of three stepping motors and the switching of the halogen lamp and also records the readings from four control thermocouples and the thermostats.
Recording of the transient flow patterns and temperature fields is performed periodically. Typically every 10-300s, short series of images are acquired and stored on the hard disk of the computer for later evaluation. The computer-controlled system of the three step-motors combined with a mirror allows to acquire images of several cross-sections, fully automatically within several seconds. Hence, due to relatively slow variations of the flow structures, transient recording of the main three-dimensional flow features is possible.

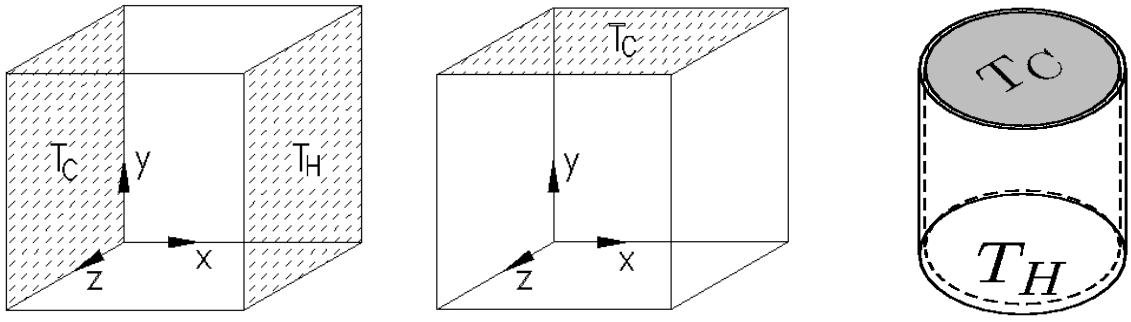


***Figure 4*** *Investigated geometry: differentially heated (a), lid cooled cube (b) and cylindrical cavity (c)*

In the experiments described here we consider natural convection of liquids in a small cubic or cylindrical cavities (Fig. 4). A typical internal dimension of the investigated flow domain is 38mm

for the cube and 37mm internal diameter and 41mm height for the cylindrical cavity. Either two opposite walls (Fig 4a) or one top wall (Fig. 4b,c) are made of metal and assumed to be isothermal. Other walls are nominally insulators of finite thermal diffusivity. They are made out of 6 and 8mm thick plexiglas or 2mm glass. The thermal conductivity of the "passive walls" seem to play an important role in the development of fine flow structures and the effect of their thickness and conductivity was investigated in different experiments [16].

Two flow configurations were considered. In the first, natural convection develops in the differentially heated cube surrounded by air (Fig. 4a). Two opposite walls are isothermal and kept at different temperatures $T_h$ and $T_c$. In the second configuration (Fig. 4b,c), the top metal wall of the cavity is isothermal at low temperature $T_c$. The other walls are non-adiabatic, allowing a heat flux from the external water bath kept at the temperature $T_h$ (see Fig. 5). Due to forced convection in the bath, it can be assumed that the temperature at the external surfaces of the cavity is close to the bath temperature. The constant temperature of the metal walls is maintained by an anti-freeze coolant flowing through the attached antechamber. The temperature of the cooling and heating liquids and that of the water in the bath (eventually surrounding the non-adiabatic walls) are controlled by two thermostats.

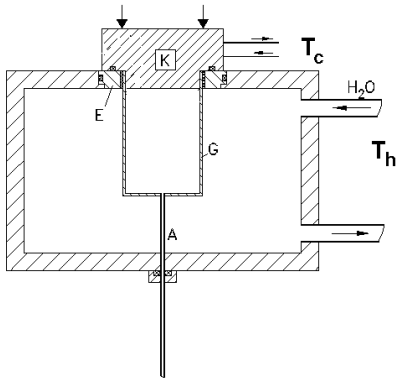


***Figure 5.*** *Lid cooled cavity, schematic of heating for the lid cooled cavity with an isothermal top lid (K) immersed in the external hot water bath*

As a flow medium, pure glycerine, its aqueous solutions and pure water were used. By varying the liquid composition and the temperature difference $\Delta T=T_h - T_c$, it was possible to cover a relatively wide range of Rayleigh and Prandtl numbers ($Ra=2.10^4$-$3.10^6$, Pr=7-6900). To investigate natural convection with phase change, distilled water was used. In that case, one of the isothermal wall was held at temperature $T_c= -10^oC$. As it is below the freezing temperature of water, ice formed there. Owing to the convective motion, the shape of the ice front is strongly non-uniform and depends on the main flow parameters and thermal boundary conditions at the "passive" side walls.

## 4. Selected results

In the following we illustrate applications of the liquid crystal tracers for a few different cases of the thermally driven flow studied in the two configurations we explained before. In all these cases, the employment of TLCs appeared to be very useful in understanding the flow structure and helped us to discover effects, which are difficult to find using point measurements. Application of the digital image analysis allowed to quantify measured temperature and velocity fields. Comparison with the numerical counterparts let us to identify discrepancies, which partly originated from the simplifications present in the numerical models.

### 4.1. Differentially heated cavity

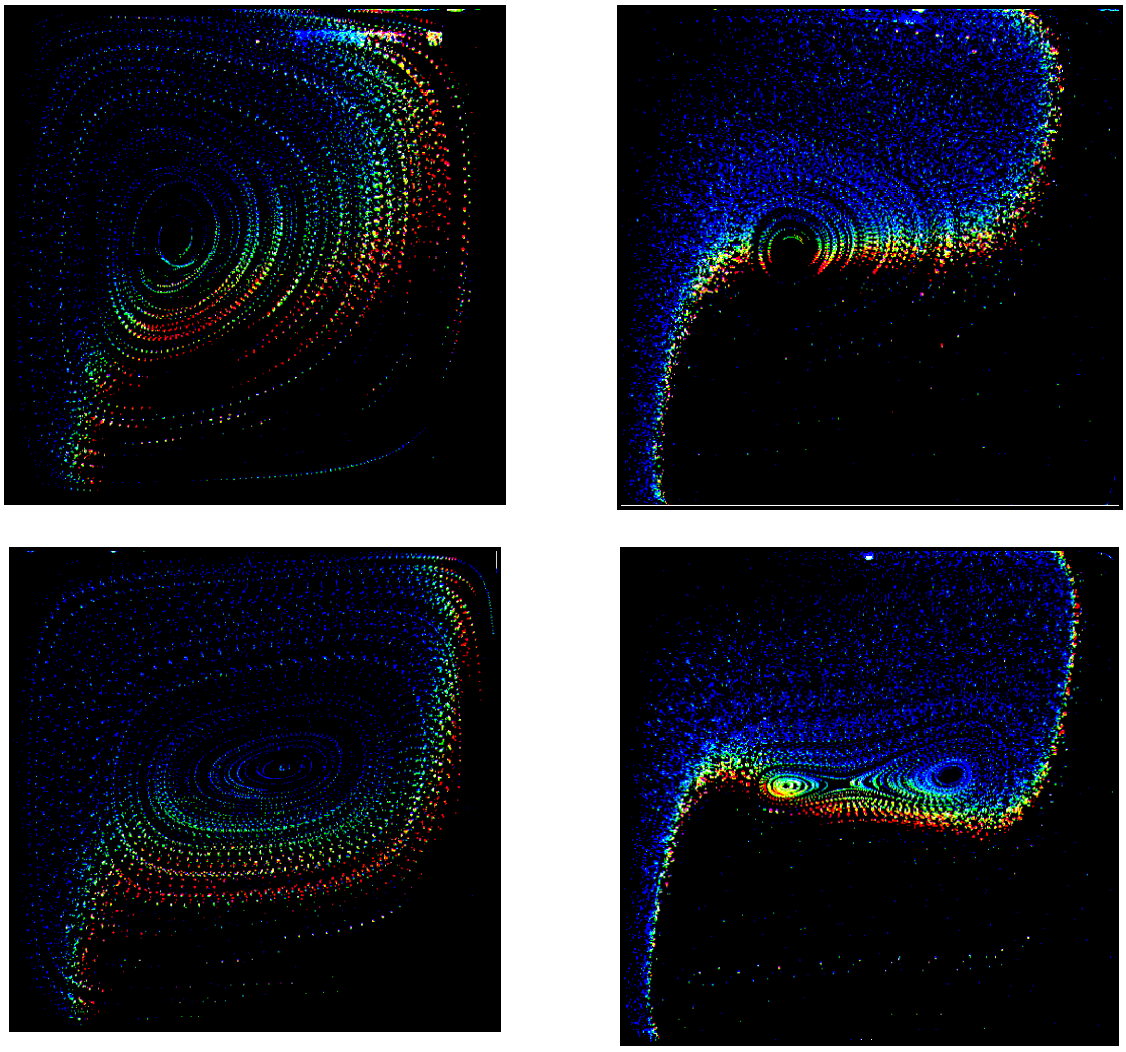

a b

***Figure 6.*** *Multiexposed photographs of liquid crystal tracers in the convective flow at the front wall z=0.95 (top row) and the centre plane z=0.5 (bottom); Pr=6300. Effect of Rayleigh number: (a) Ra=2·10$^4$, (b) Ra=8·10$^4$*

This flow configuration resembles a popular "bench mark" case, an idealised case of the flow in a cubical cavity used to test numerical solutions of the Navier-Stokes equations. The characteristic recirculating flow is generated in the cavity by the temperature gradients existing between two opposite metal walls of the cube (comp. Fig. 1). In addition to its theoretical interest, this type of convective flow has numerous potential applications, among which probably the most popular one is that of double glazing.

Initially our interest was directed towards understanding the flow in the vertical centre plane of the cavity. For this purpose, the observations of flow patterns and temperature fields were performed for several systems with increasing Rayleigh numbers from $10^4$ to $10^5$ [9]. It appeared that the flow structure in the differentially heated cavity strongly depends on the Rayleigh number. At a small Rayleigh number ($Ra<10^3$) the flow is dominated by conduction, which is seen in the form of vertical isotherms across the cavity. In the parameter range analysed ($Ra=2\cdot10^4$ - $10^5$), both convection and conduction are important. At the lower end of the range, heat transfer due to convection begins to play a significant role, generating a vertical temperature gradient in the centre of the cavity. The horizontal temperature gradient is positive everywhere, giving rise to a positive

vorticity generation. The streamlines correspond to a single roll, with its centre located at the centre of the cavity. This can be well observed in the multiexposed photographs of liquid crystal tracers conveyed by the flow (Fig. 6a). At higher Rayleigh numbers ($Ra > 6.10^4$), the horizontal temperature gradient becomes locally negative in some regions, promoting the generation of negative vorticity in the core. This causes horizontal elongation of the streamlines and the development of a second roll in the core (Fig. 6b).

As demonstrated on Fig. 1 and 6 flow visualization via liquid crystals allows to observe the flow structure and to identify variation of the temperature field. Even without quantitative data, the characteristic S-shape of the isotherms can be deduced from the colour photographs. However, the undoubted beauty of multiexposed colour photographs of liquid crystal tracers is rather useless for quantitative image analysis. Lack of particles in large regions of the flow and their individual modulation of colour are the main obstacles for a computerised analysis. Hence, the digital images of the flow taken to implement particle image velocimetry and thermometry analysis display a rather dense, uniform crowd of small, single exposed colourful dots, representing the fine dispersion of the liquid crystals material in the flow. Human eye may still easily analyse colour distribution of such images, but particle displacements can be detected only by computational means.

Figure 8 shows results of the computerised image analysis performed in the differentially heated cavity. It shows the velocity and temperature fields measured in the centre plane for the two-vortex flow configuration ($Ra=1.66 \cdot 10^5$, Pr=1109). Results are compared with their numerical counterparts [11]. Despite of the simplifications made in the numerical simulation, comparison of Fig. 8 shows that the experimental and numerical results are generally in good agreement. Small deviations in the isotherms, which are most pronounced close to the top and bottom walls, are believed to be due to the finite heat conduction within the walls, as well as to technical problems of the colour analysis close to the strongly reflecting light top wall.

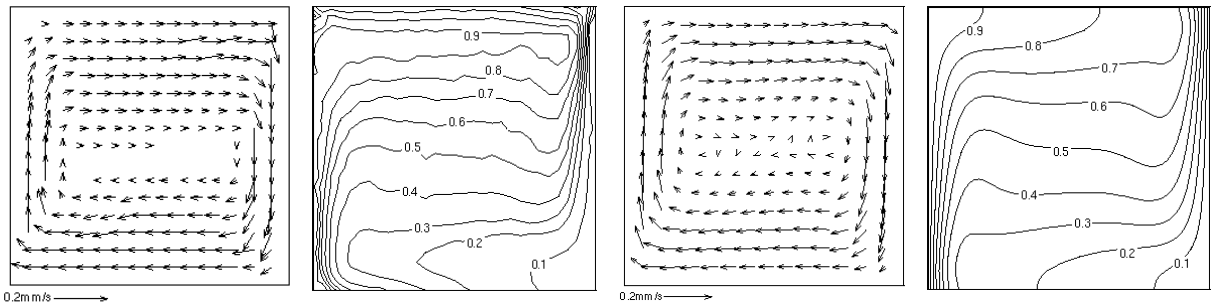


***Figure 7.*** *DPIV (a) and DPIT (b) measured velocity and temperature fields for natural convection in centre plane of differentially heated cavity; numerical counterparts (c) and (d). $Ra=1.7 \cdot 10^5$, Pr=1109*

Investigations of the onset of convection studied for a similar case [11] show particular benefits of the TLC tracers for instantaneous measurements of 2-D temperature and velocity fields. A sequence of images of the flow gives us a direct view of how, after applying a temperature jump at the hot wall, primary vertical isotherms continuously transform their shape into the final characteristic S-form (Fig. 8), generating convective flow in the whole cavity.

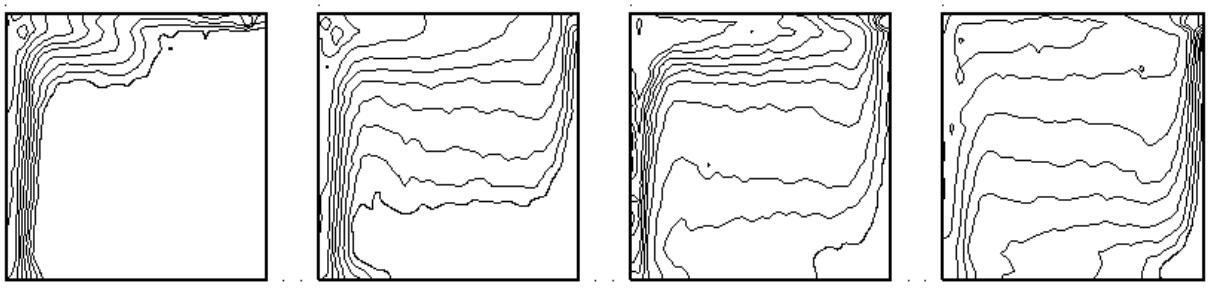

***Figure 8.*** *Transient development of isotherms measured at the centre-plane of differentially heated cavity: time t=2min, 10min, 20min and 60min after the temperature $T_h$ is applied; initial fluid temperature $T_o = T_c$; $Ra=1.8 \cdot 10^5$, Pr=980*

The good agreement observed between the calculated flow using adiabatic TBCs and the measured two-dimensional visualizations at the centre plane breaks down when approaching the front or back walls (the nominally adiabatic vertical walls) of the cavity. The single roll apparent in the two dimensional visualization (Fig. 6a), is actually a spiralling structure transporting liquid from the front and back walls into the centre and back. It was found [10] that both the experimental isotherms and the flow structure differ from those simulated for the planes out of the centre. Due to the non-adiabatic conditions on the side walls, the temperature field at those walls is characterised by larger horizontal gradients. The centre of the roll becomes shifted towards one of the isothermal walls (comp. Fig. 6). The straight inner spiral for the one roll system with an adiabatic TBCs has in reality its ends curved towards the hot wall. As for the two roll system, only one spiral initially appears at the front and back wall. It splits midway between the centre and side walls into two spirals forming characteristic "cats eyes" in the symmetry plane. The direction of the observed inner spiral is in both cases towards the centre symmetry plane. Several numerical investigations have been performed to explore this effect. It seems that the z- component of the flow velocity responsible for the three-dimensional behaviour of tracks is extremely sensitive to TBC on all non-isothermal walls. Depending on the modelled value and direction of the heat flux, the location of the core of the spirals at the side walls may be shifted towards the hot or cold side. In this way their pitch and even direction may be easily changed [18]. Because of this sensitivity, the estimation of the proper TBC for the given experiment becomes a non-trivial task, especially for the two-roll system. The trial and error method first used to fit the TBC was replaced by a process of defining an explicitly measured temperature distribution for all four non-isothermal walls. Such measurement could be done using TLCs covering inner surfaces of the cavity. For streamlines calculated with the experimentally defined wall temperatures both the direction of the calculated spirals and their pitch correlate well with the measured particle tracks [6,13]. The improvement obtained gives an indication of the necessity of modifications to the modelling of heat transport through and along non-isothermal walls.

The behaviour of natural convection of water in the vicinity of the freezing point shows an interesting feature for the typical configuration with differentially heated walls. It is mainly due to the strongly non-linear temperature dependence of the density function with the extremum at $4^oC$. The competing effects of positive and negative buoyancy force result in a flow with two distinct circulations (Figs. 9). There is a "normal" clockwise circulation, where the water density decreases with temperature (upper-left cavity region) and an "abnormal" convection with the opposite density variation and counter-clockwise rotation (lower-right region). At the upper part of the cold wall the two circulations collide with each other, intensifying the heat transfer and effectively decreasing the interface growth. Below, the convective heat transfer from the hot wall is limited by the abnormal circulation, separating it from the freezing front. Hence, the phase front is only initially flat. As time passes it deforms strongly, getting a characteristic "belly" at its lower part.

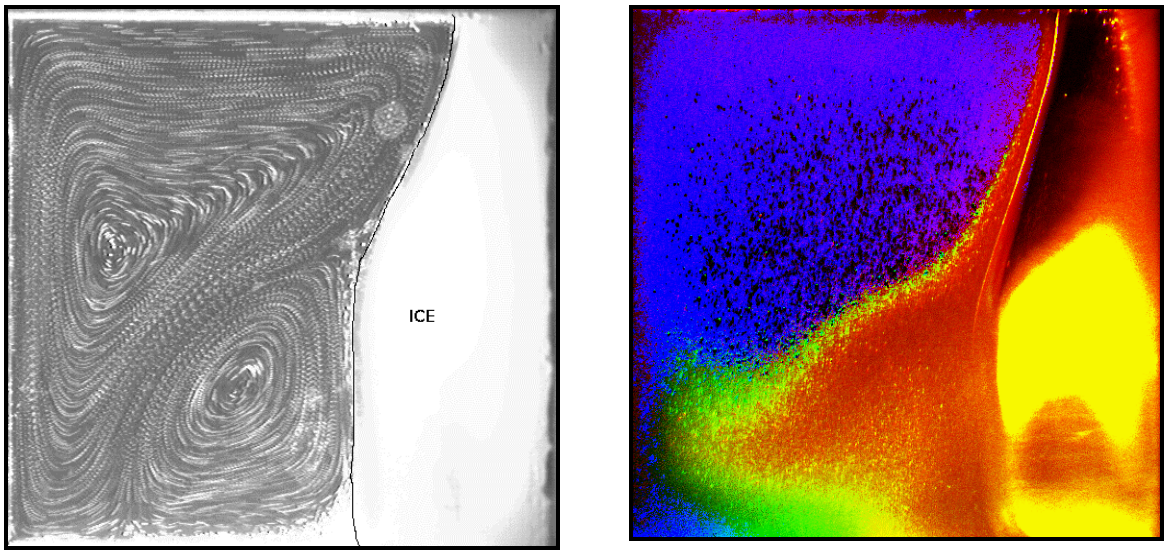


a b

***Figure 9****. Visualization of natural convection in freezing water. Particle tracks showing flow structure (a), liquid crystals tracers indicating variation of temperature (b).* $T_h$*=10°C,* $T_c$*=-10°C*

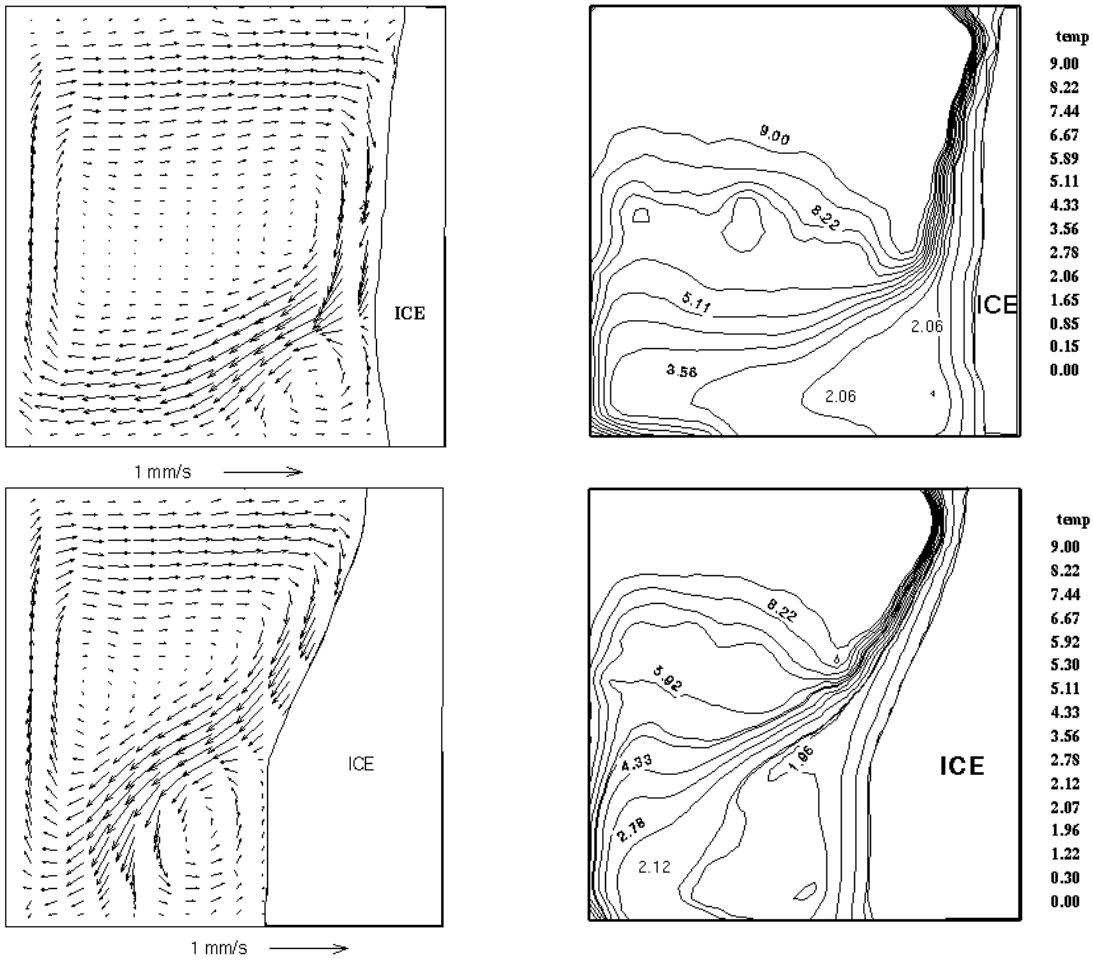


a b

***Figure 10.*** *DPIV (a) and DPIT (b) measured velocity and temperature fields for natural convection in centre plane of differentially heated cavity at 500s (top) and 3000s (bottom).* $T_h$*=10°C,* $T_c$*=-10°C;* $Ra=1.5\cdot10^6$*,* $Pr=13.3$

Digital analysis of the images seeded with liquid crystal tracers allows to describe the full transient development of the temperature and velocity fields during the freezing process. Examples of the

experimental results given here (Fig. 10) elucidate the complexity of the flow structure and its interaction with the thermal field. It is worth noting that the region separating the *normal* and *abnormal* circulations overlaps with the isotherms of the density maximum. Our numerical simulations performed for the freezing problem [14] show severe discrepancies when compared with the experimental data. It comes out that this flow structure, with the two competing circulations, is very sensitive to thermal boundary conditions at the side walls. Neither isothermal nor constant heat flux models are sufficiently accurate to reproduce the observed flow structures. Full field flow measurements led us to discover main discrepancies and indicated directions to improve the model. Despite improvements of the numerical model we used, the computational results still differ in detail from their experimental counterparts. An eventual source of the observed discrepancies could be supercooling of water, which delays creation of the first ice layer and deforms the flow pattern at the top of the cavity (comp. Movie 1). It is well known that pure water may supercool as far as -40°C, before freezing occurs. Seeding of the flow with thermochromic liquid crystals allowed us to visualize that, in fact, initial water temperature reaches about -7°C before freezing starts.

### 4.2. Lid cooled cavity

In the second configuration (comp. Fig. 5), the top wall of the cavity is isothermal at low temperature $T_c$. The other five walls are non-adiabatic, allowing a heat flux from the fluid surrounding the box. There is no well defined "hot wall" in this configuration. The temperature at the internal surfaces of the cavity adjusts itself depending on both the flow and the heat flux through and along the walls. To define non-dimensional parameters describing flow, the external temperature $T_h$ is used to calculate the temperature difference.

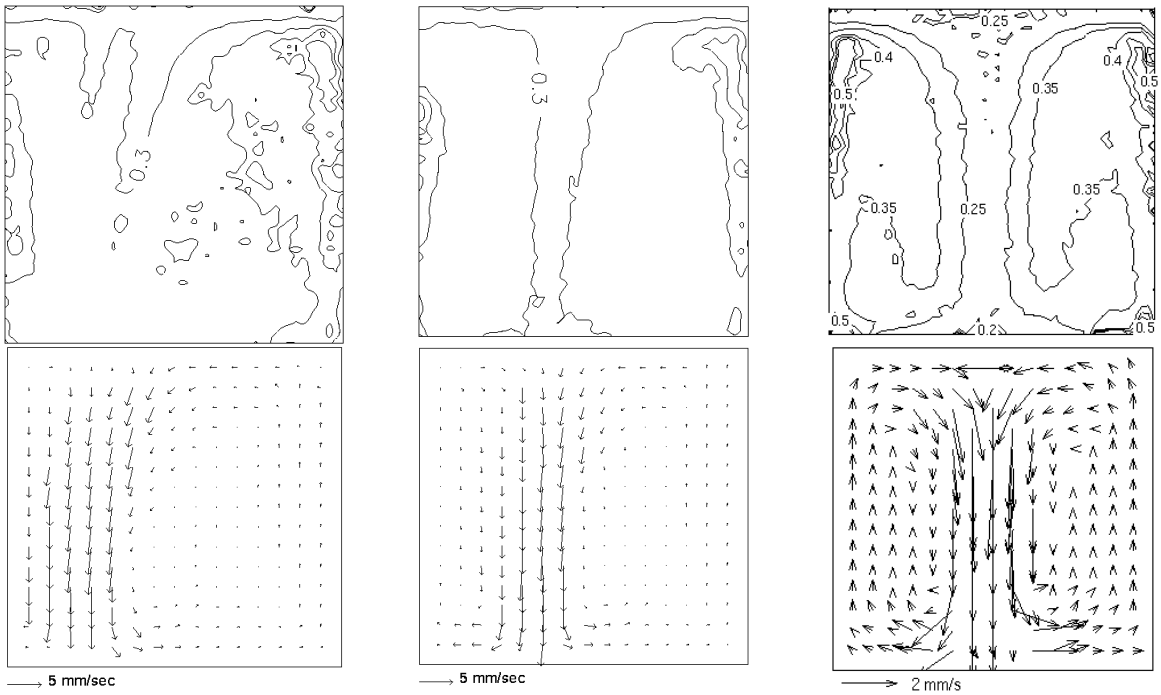


***Figure 11.*** *Typical instabilities observed during the onset of convection: temperature (upper row) and velocity (bottom row) fields measured by DPIV & T for the centre plane of the cube shaped cavity made of plexiglas; $T_h$=21°C, $T_c$=15°C, Ra=2.7·10$^6$, Pr=8*

The lid cooled cavity was selected to investigate the convective flow with and without a phase change (freezing of water at the top wall). When the phase change occurs, it resemble to some extent a directional solidification in a Bridgman furnace used for crystal growth.
Physically this configuration bears some similarity to the Rayleigh-Bénard problem. However, due to altered thermal boundary conditions at the side walls, the flow structure is different. For the cube shaped cavity as well as in the cylinder, symmetry of the enclosure imposes a strong downward flow along the vertical axis of symmetry. However, before a stable final flow structure is achieved, several oscillatory changes in its pattern are observed. The initial flow instabilities are well seen in temperature and velocity fields visualized in the box (Figure 11). Numerical simulations confirmed this instability [1]. It appears that the initial cold thermal boundary layer at the lid is unstable and breaks down to several plumes falling down along the side walls. Depending on experimental disturbances or numerical noise present, the flow pattern exhibits several strongly asymmetrical transitions before a final configuration with a single cold "jet" along the cavity axis and a reverse flow along side walls establishes. A similar instability is observed by the onset of convection in the cylindrical cavity.

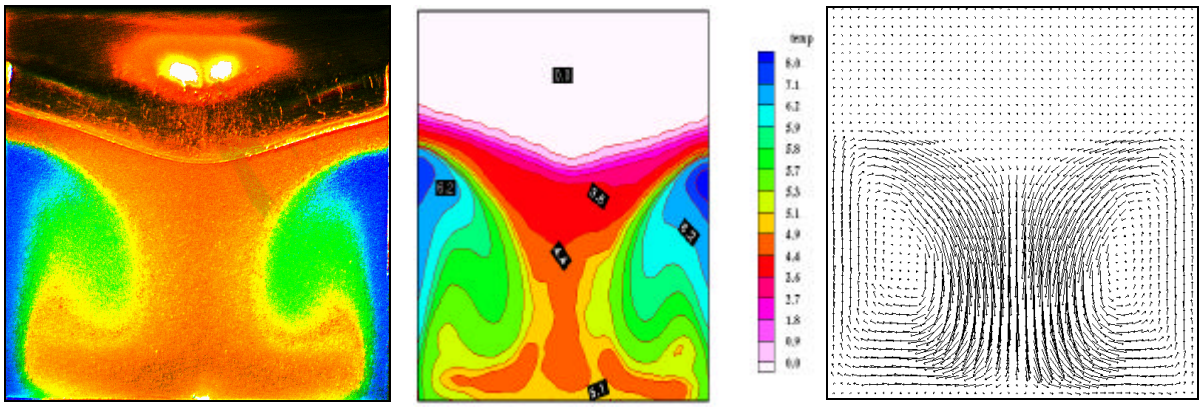


***Figure 12*** *Freezing of water from the top in the lid cooled cavity. Recorded image of TLC tracers (a), evaluated temperature (b) and velocity (c) fields. Time step - 3600s after cooling starts;* $T_c$*= -10°C,* $T_{ext}$*= 20°C,* $Ra=3\cdot10^6$*, Pr=13.3*

The formation of ice has been studied by decreasing the lid temperature down to -10°C. A complicated flow pattern which establishes, becomes visible also in the structure of the ice surface. It was found that the creation of the ice layer at the lid has a stabilising effect on the flow. This follows from the symmetry of the ice solid surface, which imposes the direction and character of the flow, eliminating the instabilities observed in the pure convection case. There is also a density inversion under the lid which decelerates the main "jet" and limits a strong generation of vorticity in that region.
Due to the stochastic development of the flow pattern, direct comparison of transient experimental and numerical results becomes difficult at early time steps. Hence, to minimise uncertainty of the initial conditions a second set of investigations was performed. We call it the „warm start", because the freezing starts after a steady convection pattern is established in the cavity. This initial flow state corresponds to natural convection without phase change, with the lid temperature set to 0°C. Movie 2 displays the experimental result of the freezing process which starts from the developed natural convection. Regular flow pattern is seen, with the central, stable cold jet at the cavity axis. Figure 12 shows the temperature and velocity field evaluated at the time step 3600s for this case.
The flow visualisation performed in the cube shaped cavity shows that the flow observed in the

centre plane, transporting fluid upwards along the side walls and downwards in a central cold jet along the cavity axis, in fact consists of the a complex spiralling structure in three-dimensions. Depending on the thermal boundary conditions at the side walls different configurations are realised by the flow. For walls of high heat conductivity (glass), eight symmetric cells are created by the flow. For Plexiglas walls, additional small recirculation regions appear, separating the main cells. The flow structure is also manifested in the complex structure of the ice surface. Both in the computed and observed ice surface, a star-like grooving reflects the eight-fold symmetry of the flow. A colour play of TLCs-seeded flow images taken directly under the lid (Fig. 13a, b) shows differences of flow structures in the temperature pattern. It appears, that only a slight change of the *thermal boundary conditions* at the side walls may modify the flow pattern. This was observed by replacing the side walls of low conductivity Plexiglas with thin glass walls.

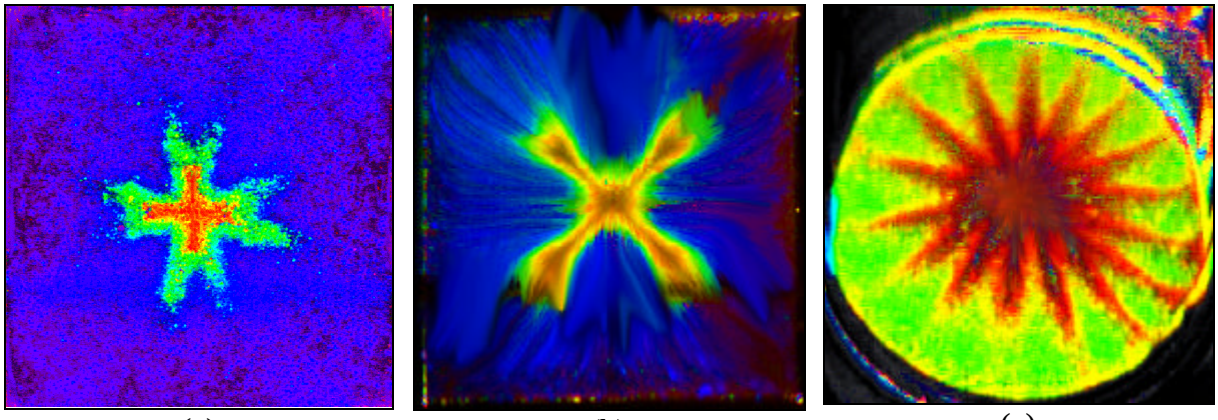

(a) (b) (c)

***Figure 13****. Natural convection in the lid cooled cavities. Temperature distribution recorded with help of TLC directly under the cooled top wall. Effect of the walls properties on the flow structure visible in the temperature fields: (a) - plexiglas walls, (b) - glass walls, (c) - cylindrical glass cavity*

Initially our numerical simulations of the flow with simple, heat flux based thermal boundary conditions at the side walls, have shown discrepancies [1]. Although the computational results confirmed the eight-fold symmetry of the temperature and flow fields experimentally observed, their orientation was different. Moreover, the measured isotherms were evidently shifted to higher values. Quantitative differences were noticed in the temperature distribution observed at the horizontal cross-section. It was found that the heat flux through and along the walls has to be incorporated to the numerical model. Inclusion of the side walls in the computational domain and solving the coupled fluid-solid heat conduction problem improved the agreement with the observed flow pattern. Also the observed temperature distribution as well as its symmetry were fully recovered in the numerical results [16,18]. It was only as a result of using *both* the experimental and numerical methods that the fine structures of the thermal flow were fully understood.

An interesting example of the temperature pattern observed in the cylindrical cavity is shown in Fig. 13c. Despite the cylindrical symmetry, azimuthal flow structures appear, dividing the flow domain into regular sequence of 16-18 radial running rolls. This fact was recently confirmed in the numerical simulations. The experimental evidence of this flow symmetry breaking was only possible with help of TLCs visualisation method. It is interesting to note that these structures remain when the phase change takes place [16]. Characteristic star-like grooves in the ice surface growing at the lid follow the temperature field visualized with TLCs.

## 5. Conclusions

A new experimental technique, in this case true-colour image processing of liquid crystal patterns, allows new approaches to old problems and, at the same time, opens up new areas of research. Image processed data makes available quantitative, full-field information about the temperature and velocity fields, which will undoubtedly encourage the study of situations which have been, until now, too complex to consider. The non-invasive character of the method and its relative simplicity offers valuable tool for the full field verification and validation of numerical results.


## Acknowledgements

This is a summary of the work which the author has been fortunate to share with his colleagues and students, first at the Max-Planck-Institut and presently at his home institution. In particular I would like to acknowledge the contribution of W. Hiller, St. Koch, C. Abegg, C. Söller, A. Cybulski and M. Rebow, to what has been a team effort over a number of years.


## 6. References*


**[1]** **Abegg, C., De Vahl Davis, G., Hiller, W.J., Koch, St., Kowalewski, T.A., Leonardi, E., Yeoh, G.H.** *Experimental and numerical study of three-dimensional natural convection and freezing in water*. Proc. of 10th Int. Heat Transfer Conf., Brighton, **4**, pp.. 1-6, 1994.

**[2]** **Bonnett, P. Jones, T.V., Donnell, D.G.** *Shear-stress measurement in aerodynamic testing using cholesteric liquid crystals.* Liquid Crystal **6**, pp.271-280, 1989

**[3]** **Dabiri, D., Gharib, M.** *Digital particle image thermometry: The method and implementation.* Exp. in Fluids **97**, pp.77-86, 1991.

**[4]** **Goh, L.P., Leonardi, E. & de Vahl Davis, G.** *FRECON3D -Users Manual. A program for the numerical solution of mixed convection in a three-dimensional rectangular cavity.* Report 1988/FMT/7, University of New South Wales, Sydney 1988.

**[5]** **Hay J.K., Hollingsworth D.K.** *A comparison of trichromic systems for use in the calibration of polymer-dispersed thermochromic liquid crystals*. Exp. Thermal Fluid Scs, **12**, pp. 1-12, 1996.

**[6]** **Hiller W.J., Koch, St., Kowalewski, T.A., Mitgau, P., Range, K.** *Visualization of 3-D natural convection*, in Flow Visualization VI, Eds. Tanida Y. & Miyashiro H., pp 674-678, Springer-Verlag, 1992.

**[7]** **Hiller, W., Kowalewski, T.A**. *Simultaneous measurement of the temperature and velocity fields in thermal convective flows*, in Flow Visualization IV, Ed. Claude Veret, pp. 617-622, Hemisphere, Paris, 1987.

**[8]** **Hiller, W.J., Koch, St., Kowalewski, T.A.** *Simultane Erfassung von Temperatur- und Geschwindigkeits-feldern in einer thermischen Konvektionsströmung mit ungekapselten Flüssigkristalltracern*, in: 2D-Meßtechnik DGLR-Workshop, Markdorf, DGLR-Bericht 88-04, pp. 31 - 39, DGLR Bonn, 1988.

**[9]** **Hiller, W.J., Koch, St., Kowalewski, T.A.** *Three-dimensional structures in laminar natural convection in a cube enclosure*, Exp. Therm. and Fluid Sci. **2**, pp 34-44, 1989.

**[10]** **Hiller, W.J., Koch, St., Kowalewski, T.A., De Vahl Davis, G., Behnia, M.** *Experimental and numerical investigation of natural convection in a cube with two heated side walls, in* Proc.of IUTAM Symposium, Cambridge UK, Edits. H.K. Moffat & A. Tsinober, pp 717 - 726, CUP 1990.

**[11]** **Hiller, W.J., Koch, St., Kowalewski, T.A. & Stella, F.** *Onset of natural convection in a cube*, Int. J. Heat Mass Transfer, **36**, pp 3251-3263, 1993.

**[12]** **Hollingsworth, D.K. Boehman, A.L. Smith, E.G, Moffat, R.J.** *Measurement of temperature and heat transfer coefficient distributions in a complex flow using liquid crystal thermography and true-colour image processing* ASME J.Heat Transfer **123**, pp. 35-42, 1989.


*Examples of colour images and some references can be found at the Web page: http://www.ippt.gov.pl/~tkowale/

**[13]** **Koch, St.** *Berührungslose Messung von Temperatur und Geschwindigkeit in freier Konvektion,* Ph.D. Thesis in Mitteilungen aus dem MPI 108, Göttingen, 1993.

**[14]** **Kowalewski T.A., Rebow M.** *Freezing of water in the differentially heated cubic cavity,* Int. J. Comp. Fluid Dyn. **11,** 193-210, 1999.

**[15]** **Kowalewski, T. A. Cybulski A.** *Experimental and numerical investigations of natural convection in freezing water,* Int. Conf. on Heat Transfer with Change of Phase, Kielce, in Mechanics vol. **61**/2, pp. 7-16, 1996.

**[16]** **Kowalewski, T. A. Cybulski A.** *Natural convection with phase change,* IPPT Reports **8**/97, IPPT PAN Warszawa 1997.

**[17]** **Quénot G., Pakleza J., Kowalewski T.A.** *Particle Image Velocimetry with Optical Flow,* Experiments in Fluids **25**, pp. 177-189, 1998.

**[18]** **Söller C., Hiller W.J., Kowalewski T.A. & Leonardi E.** *Experimental and numerical investigation of convection in lid cooled cavities - effects of non-ideal thermal boundary conditions on three-dimensional flow, paper presented* at 3rd ICIAM Congress, Hamburg 1995.

**[19]** **Stasiek J.** *Thermochromic liquid crystals and true colour image processing in heat transfer and fluid-flow research,* Heat Mass Transf. **33**, 27-29, 1997.

**[20]** **Straley S.M.J.** *Physics of Liquid Crystals.* Review of Modern Physics **46**/4 pp. 617-704, 1974,

**[21]** **Westerweel J.** *Digital Particle Image Velocimetry - Theory and Application*, Delft, Delft University Press 1993.

**[22]** **Yeoh. G.H.,** *Natural convection in a solidifying liquid,* Ph.D. Thesis, University of New south Wales, 1993.

**[23]** **Zhang, X. Stasiek, J. And Collins, M.W.** *Experimental and numerical analysis of convective heat transfer in turbulent channel flow with square and circular columns.* Exp. Thermal Fluid Science **10**, pp. 229-237, 1995.

## Movies:

***Movie 1.*** *Ice front observed in differentially heated cavity during 3000s period. Initial supercooling of water visible.* $T_h=10^oC$, $T_c=-10^oC$. *Temperature visualized by TLC tracers.*

***Movie2:*** *Ice front in lid cooled cavity observed during 3600s, freezing starts from developed convection flow. Plexiglas cavity,* $T_h=20^oC$, $T_c=-10^oC$ *(comp. Fig. 12).*